Enhancement of Spin Correlation in Cr_2O_3 Film Above Néel Temperature Induced by Forming a Junction With Fe_2O_3 Layer: First-Principles and Monte-Carlo Study

Yohei Kota[1], Hiroshi Imamura[1], and Munetaka Sasaki[2]

[1]Spintronics Research Center, National Institute of Advanced Industrial Science and Technology, Tsukuba 305-8568, Japan
[2]Department of Applied Physics, Tohoku University, Sendai 980-8579, Japan

We propose an approach to enhance the antiferromagnetic spin correlation in the Cr_2O_3 film by forming a junction with the Fe_2O_3 layer. First-principles calculations and Monte-Carlo simulations were performed to evaluate the exchange coupling constant between the Cr and Fe spin and the spin correlation functions of the Fe_2O_3/Cr_2O_3 bilayer system in a finite temperature. We found that above the Néel temperature of Cr_2O_3, the length of the antiferromagnetic spin correlation in the bilayer system is increased by more than twice as that of the bulk system.

Index Terms— **Classical Heisenberg model, Cr_2O_3, Fe_2O_3, first-principles calculation, Monte-Carlo simulation, spin correlation.**

I. Introduction

MAGNETOELECTRIC materials have attracted much attention as a basic element of low power consumption memories. One of the promising magnetoelectric materials is antiferromagnetic Cr_2O_3, and since the 1960s much effort has been devoted to studying its magnetic and electronic properties. Recently, the electric field control of exchange bias was demonstrated in the Cr_2O_3/Co bilayer system [1], [2], and magnetoelectric effect was also observed for the Cr_2O_3/Fe_2O_3 ultrathin film (∼1 nm) [3]. These reports brought significant progress in realizing magnetoelectric spintronics devices [4]–[6]. However, for practical application, it is necessary to enhance the antiferromagnetic spin correlation of Cr_2O_3 whose Néel temperature is 308 K [7] for bulk samples. To enhance the Néel temperature, there are several theoretical proposals, such as B-doping and strain engineering [8]–[10], predicting a 10%–20% enhancement.

In this paper, we propose another approach to maintain the antiferromagnetic spin correlation in Cr_2O_3 film above the Néel temperature: Cr_2O_3 and Fe_2O_3 film junction. Since the Néel temperature of Fe_2O_3 is as high as 950 K [12], its antiferromagnetic order survives above the Néel temperature of Cr_2O_3. Therefore, by implementing a junction between Cr_2O_3 and Fe_2O_3, we can expect the retention in antiferromagnetic correlation of Cr spin near the interface even above the Néel temperature of Cr_2O_3, with reference to a previous study concerning the transition temperature of magnetic thin films caused by the proximity effects [13], [14]. To confirm the feasibility of this approach, we performed numerical simulations on the basis of the first-principle calculations and Monte-Carlo simulations to evaluate the spin correlation in a Cr_2O_3 layer above the Néel temperature. We found that the length of the antiferromagnetic correlation in Cr_2O_3 near the interface of an Fe_2O_3/Cr_2O_3 bilayer system is increased compared with Cr_2O_3 bulk system.

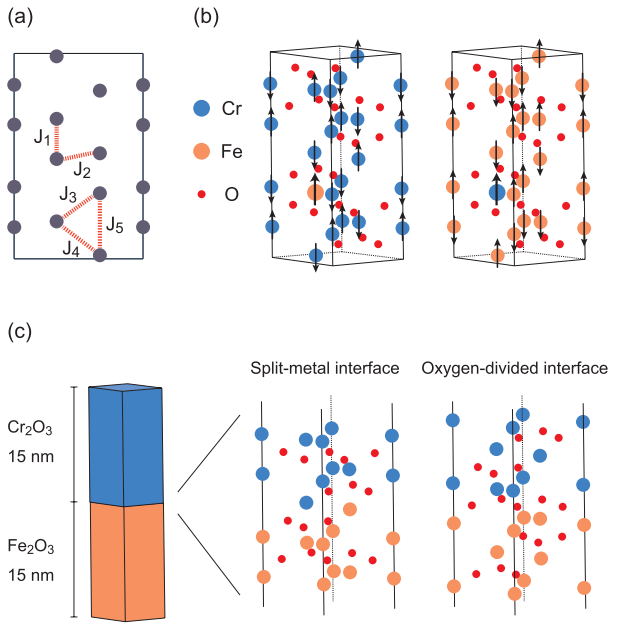

Fig. 1. (a) Exchange interactions and coupling constants up to the fifth-nearest neighbors, J_1–J_5, in the corundum-type lattice. The unit cell is projected on (110)-plane. (b) Crystal structure and spin configuration in Fe-doped Cr_2O_3 ($Cr_{11}Fe_1O_{18}$) and Cr-doped Fe_2O_3 ($Cr_1Fe_{11}O_{18}$) with the corundum-type structure. (c) Schematic of the bilayer structure of Fe_2O_3/Cr_2O_3 used to perform the Monte-Carlo simulation. Two types of interface structures, oxygen-divided and split-metal, were considered.

II. Calculation Details

First-principles calculations of electronic structure and exchange coupling constant were performed using the Vienna ab initio simulation package (VASP) [15], [16]. We evaluated the exchange coupling constant up to the fifth-nearest neighbors, J_1–J_5, in the corundum-type structure as shown in Fig. 1(a). The exchange coupling constants are evaluated by

Manuscript received March 7, 2014; revised May 1, 2014; accepted May 10, 2014. Date of current version November 18, 2014. Corresponding author: H. Imamura (e-mail: h-imamura@aist.go.jp).

Color versions of one or more of the figures in this paper are available online at http://ieeexplore.ieee.org.

Digital Object Identifier 10.1109/TMAG.2014.2324014

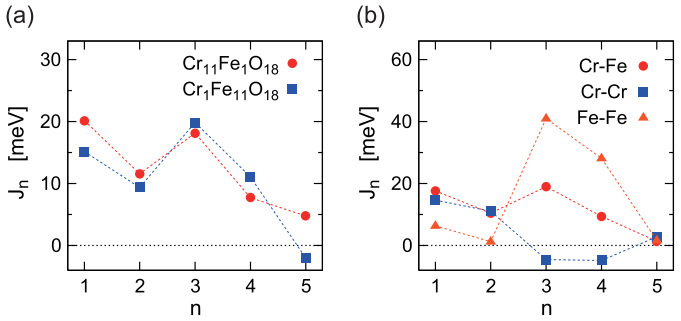

Fig. 2. (a) Exchange coupling constants up to the fifth-nearest neighbors, J_1–J_5, between Cr–Fe spins. Two results obtained from $Cr_{11}Fe_1O_{18}$ and $Cr_1Fe_{11}O_{18}$ are shown. (b) J_1–J_5 of Cr–Fe spin pairs, which are the average of the two results shown in (a). J_1–J_5 of Cr–Cr and Fe–Fe spin pairs [9] are also shown.

fitting the energy of the ground state and exited states with a noncollinear spin configuration. Other details of the calculation setups and method to evaluate the exchange coupling constants were explained in our previous papers [9], [10]. To calculate the exchange coupling constants in the corundum-type lattice, we selected Fe-doped Cr_2O_3 ($Cr_{11}Fe_1O_{18}$) and Cr-doped Fe_2O_3 ($Cr_1Fe_{11}O_{18}$) as shown in Fig. 1(b). We considered the on-site Coulomb interaction correction; U–J parameters were set to 3.2 eV for d-orbital of Cr and 4.3 eV for d-orbital of Fe [11].

Monte-Carlo simulations were also performed to analyze spin correlation at a finite temperature. We adopted the classical Heisenberg model of corundum-type Fe_2O_3/Cr_2O_3 bilayer system

$$\mathcal{H}_{\rm Spin} = \sum_{\langle i,j\rangle} J^{\rm Fe\text{–}Fe}_{\langle i,j\rangle} \boldsymbol{S}_i \cdot \boldsymbol{S}_j + \sum_{\langle k,\ell\rangle} J^{\rm Cr\text{–}Cr}_{\langle k,\ell\rangle} \boldsymbol{S}_k \cdot \boldsymbol{S}_\ell + \sum_{\langle i,k\rangle} J^{\rm Cr\text{–}Fe}_{\langle i,k\rangle} \boldsymbol{S}_i \cdot \boldsymbol{S}_k \quad (1)$$

using the exchange coupling constants between Cr–Fe, Cr–Cr, and Fe–Fe spins ($J^{\rm Cr\text{–}Fe}$, $J^{\rm Cr\text{–}Cr}$, and $J^{\rm Fe\text{–}Fe}$). Note that i and j (k and ℓ) denote Fe (Cr) site index, and $\boldsymbol{S}_i$ is the unit vector of the spin direction at the i-site. We adopted Fe_2O_3 (15 nm)/Cr_2O_3 (15 nm) layered structure and considered split-metal and oxygen-divided interfaces [19], as shown in Fig. 1(c). The outer ends of the Fe_2O_3 and Cr_2O_3 layers were treated as a vacuum surface. The spin correlation function $\langle \boldsymbol{S}_0 \cdot \boldsymbol{S}_m \rangle_T$ between Fe and Cr spins in the corundum-type lattice was calculated, where m and T stand for the site index and temperature. The spin-realignment (Morin) transition in Fe_2O_3 was neglected, because it can be suppressed by a small amount of Rh or Ir doping [17], [18].

III. Results and Discussion

A. Exchange Coupling Constants

Fig. 2(a) shows the exchange coupling constants up to the fifth-nearest neighbors J_1–J_5 between Cr and Fe spins in $Cr_{11}Fe_1O_{18}$ and $Cr_1Fe_{11}O_{18}$, obtained from the first-principles calculations. The positive (negative) sign of the coupling constants indicates antiferromagnetic (ferromagnetic) interaction. In Fig. 2(a), we see that the n dependence of the exchange coupling constants J_1–J_4 of $Cr_{11}Fe_1O_{18}$ and $Cr_1Fe_{11}O_{18}$ shows the same trend with respect to the signs and magnitudes. The signs of J_1–J_4 are positive, and this result is consistent with the previous work [20]. One can see that there exists the following relation among the absolute values, $|J_1| \approx 2|J_2| \approx |J_3| \approx 2|J_4|$, although the compositions of Cr and Fe are different in these systems.

The exchange coupling constants of Cr–Fe spin pairs at the Fe_2O_3/Cr_2O_3 interface are basically determined by their relative position, if the corundum-type interface structure as shown in Fig. 1(c) is realized. Fig. 2(b) shows the J_1–J_5 values of Cr–Fe spin pairs, in addition to those of Cr–Cr and Fe–Fe spin pairs calculated in our previous work [9]. We notice that the exchange coupling constants obtained from first-principles calculations shown in Fig. 2(b) are consistent with the Kanamori–Goodenough (KG) rule [21], [22], which provides the semiquantitative description of the exchange interaction in transition metal oxides. In the KG rule, the exchange coupling constants are determined by the relative position (coupling angle via oxygen) of atoms and their electron configurations (atomic species). In the corundum-type lattice, the coupling angle of the J_1 and J_2 (J_3 and J_4) spin pair is about 90 degree (135 degree). The electron configurations of Cr^{3+} and Fe^{3+} ion are $3d^3$ and $3d^5$ with a high-spin state, respectively. According to the KG rule, the J_1–J_4 values of Cr–Fe spin pairs indicate antiferromagnetic interaction and the absolute values are approximately comparable, that is, $|J_1|, |J_2| \approx |J_3|, |J_4|$ (actually $|J_1| \approx 2|J_2|$ and $|J_3| \approx 2|J_4|$ because of the difference in their intersite distance). Also, the KG rule provides $|J_1|, |J_2| > |J_3|, |J_4|$ for Cr–Cr spin pairs and $|J_1|, |J_2| < |J_3|, |J_4|$ for Fe–Fe spin pairs, as discussed in [9].

B. Spin Correlation Functions

In this section, the spin correlation function in the Fe_2O_3/Cr_2O_3 bilayer system was investigated on the basis of the classical Heisenberg model. We used the exchange coupling constants of Cr–Cr, Fe–Fe, and the Cr–Fe spin pairs obtained from first-principles calculations and performed Monte-Carlo simulations. Let us first look into the magnetic structure in the ground state of the Fe_2O_3/Cr_2O_3 bilayer system before presenting spin correlation functions. Fig. 3(a) and (b) show the temperature dependence of the thermal average of the normalized staggered magnetization $\langle |\boldsymbol{M}_{\rm Stg}| \rangle_T / \langle |\boldsymbol{M}_{\rm Stg}| \rangle_{T=0}$,[1] which is an order parameter of antiferromagnets, inside the Cr_2O_3 and Fe_2O_3 layer. The region 1 nm or more from the interface was considered in the calculation. Fig. 3(c) and (d) shows the ground state magnetic structure near the interface of Fe_2O_3/Cr_2O_3.

The magnetic structures of the Fe_2O_3 and Cr_2O_3 layer inside the region (1 nm or more from the interface) correspond to those of the classical ground state of the bulk. In Fig. 3(a) and (b), $\langle |\boldsymbol{M}_{\rm Stg}| \rangle_T / \langle |\boldsymbol{M}_{\rm Stg}| \rangle_{T=0}$ of Cr_2O_3 and

[1] Staggered magnetizations of Cr_2O_3 and Fe_2O_3 are defined as $\boldsymbol{M}_{\rm Stg} = \boldsymbol{\mathcal{S}}_{(1)} - \boldsymbol{\mathcal{S}}_{(2)} + \boldsymbol{\mathcal{S}}_{(3)} - \boldsymbol{\mathcal{S}}_{(4)}$ and $\boldsymbol{M}_{\rm Stg} = \boldsymbol{\mathcal{S}}_{(1)} - \boldsymbol{\mathcal{S}}_{(2)} - \boldsymbol{\mathcal{S}}_{(3)} + \boldsymbol{\mathcal{S}}_{(4)}$, respectively. Here, $\boldsymbol{\mathcal{S}}_{(n)}$ (n = 1–4) is the summation of spin at four equivalent positions in the primitive cell of corundum-type crystal [see Fig. 1(a) in [9]].

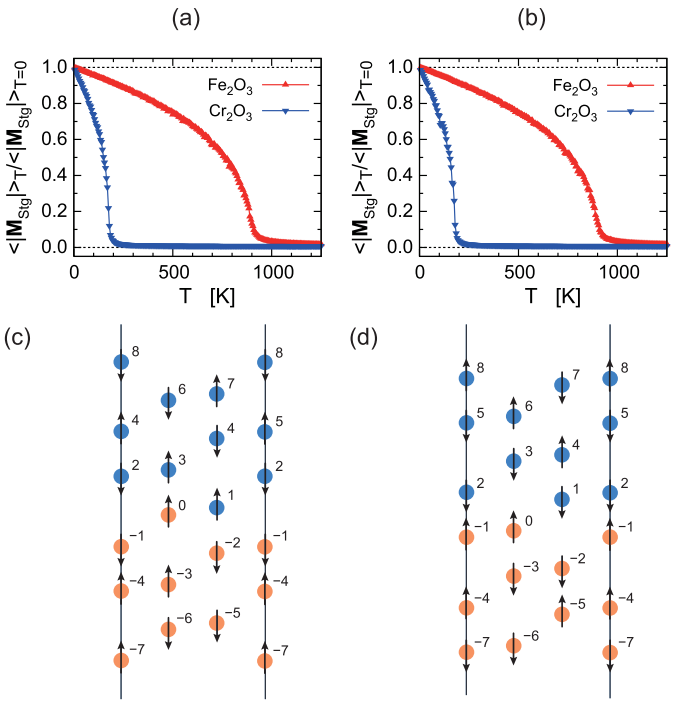

Fig. 3. Normalized staggered magnetization $\langle|\boldsymbol{M}_{\rm Stg}|\rangle_T/\langle|\boldsymbol{M}_{\rm Stg}|\rangle_{T=0}$ inside the Cr_2O_3 and Fe_2O_3 layer as a function of temperature T for (a) the split-metal interface and (b) the oxygen-divided interface. The ground state magnetic structure around Fe_2O_3/Cr_2O_3 for the split-metal and oxygen-divided interface are shown in (c) and (d), respectively.

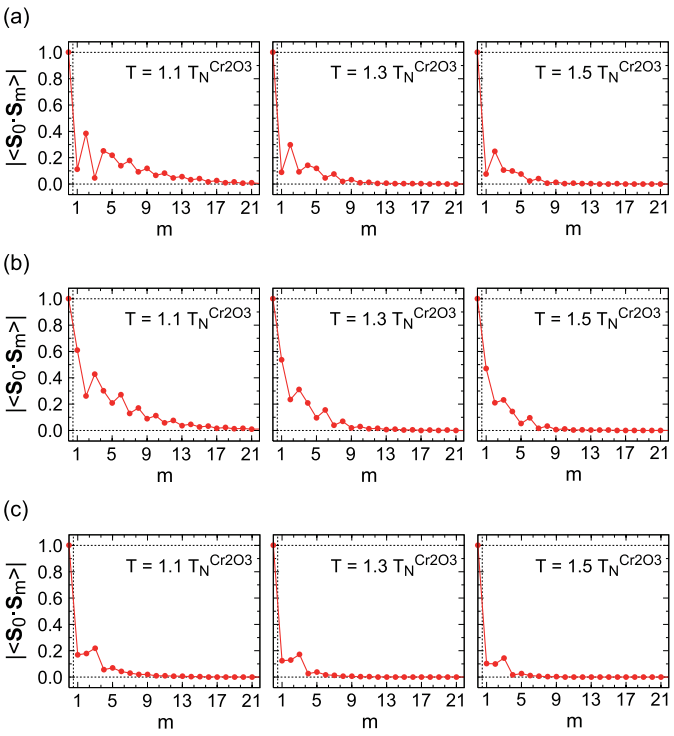

Fig. 4. (a) Calculated spin correlation function between the interfacial Fe ($m = 0$) and Cr ($m > 0$) spins, $|\langle \boldsymbol{S}_0 \cdot \boldsymbol{S}_m\rangle_T|$, at $T = 1.1\ T_{\rm N}^{\rm Cr_2O_3}$, $1.3\ T_{\rm N}^{\rm Cr_2O_3}$, and $1.5\ T_{\rm N}^{\rm Cr_2O_3}$ for the Fe_2O_3/Cr_2O_3 bilayer with split-metal interface. (b) Similar plot for the Fe_2O_3/Cr_2O_3 bilayer with oxygen-divided interface. (c) Calculated spin correlation function between the Cr spins in bulk Cr_2O_3.

Fe_2O_3 changes from zero to finite values around the Néel temperature, $T_{\rm N}^{\rm Cr_2O_3} = 177$ K and $T_{\rm N}^{\rm Fe_2O_3} = 901$ K, respectively, which were previously calculated for the bulk materials (the calculated Néel temperature of Cr_2O_3 is about 60% of experimental value) [9]. Below the Néel temperature, the $\langle|\boldsymbol{M}_{\rm Stg}|\rangle_T/\langle|\boldsymbol{M}_{\rm Stg}|\rangle_{T=0}$ values approach 1 with decreasing T; therefore, the ground state magnetic structures of the Fe_2O_3 and Cr_2O_3 layer inside the region are similar to that of the bulk materials in both cases of the oxygen-divided and split-metal interface.

In contrast to the layer inside region, the magnetic structure near the interface of Fe_2O_3/Cr_2O_3 is different from the bulk, especially in the case of the oxygen-divided interface. In Cr_2O_3 (Fe_2O_3) bulk, Cr (Fe) spins align antiparallel (parallel) in Cr (Fe) two atomic layers [$m = 2m' - 1$ and $2m'$ (m': integer) in Fig. 3(c) and (d)], which are sandwiched by O layers. The magnetic structure near the split-metal interface [Fig. 3(c)] is similar to that of the Cr_2O_3 and Fe_2O_3 bulk. On the other hand, the magnetic structure of Cr_2O_3 at the oxygen-divided interface [Fig. 3(d)] is different from that of the bulk, that is, Cr spins at the interface align parallel in Cr at two atomic layers ($m = 1$ and 2), since Cr spin at $m = 2$ is reversed by strong antiferromagnetic interactions with Fe spin at $m = 0$ via $J_4^{\rm Cr\text{–}Fe}$ and Fe spin at $m = -1$ via $J_1^{\rm Cr\text{–}Fe}$.

In the vicinity of the Fe_2O_3/Cr_2O_3 interface, magnetic frustration is caused by the competition of exchange interactions. In the split-metal interface, Fe spin at $m = 0$ and Cr spin at $m = 1$, and Fe spin at $m = 0$ and Cr spin at $m = 3$ align parallel [Fig. 3(c)] despite antiferromagnetic $J_2^{\rm Cr\text{–}Fe}$ and $J_1^{\rm Cr\text{–}Fe}$ interaction, respectively, as shown in Fig. 2(b). Similarly, in the oxygen-divided interface, Cr spins at $m = 1$ and 2 align parallel [Fig. 3(d)] despite the antiferromagnetic $J_2^{\rm Cr\text{–}Cr}$ interaction. It is difficult to satisfy the balance among all exchange interactions because of the complex competition.

Next, we present spin correlation between Fe_2O_3 and Cr_2O_3 layers above the Néel temperature of Cr_2O_3. Fig. 4(a) and (b) shows the absolute values of the thermal average of the spin correlation function $|\langle \boldsymbol{S}_0 \cdot \boldsymbol{S}_m\rangle_T|$ between the interfacial Fe ($m = 0$) and Cr ($m > 0$) in the split-metal and oxygen-divided interface, respectively. The spin correlation function of bulk Cr_2O_3 are also shown in Fig. 4(c) for comparison. In these figures, the temperature is normalized by $T_{\rm N}^{\rm Cr_2O_3}$.

The $|\langle \boldsymbol{S}_0 \cdot \boldsymbol{S}_m\rangle_T|$ values in Fig. 4 clearly show that the spin correlation in the Cr_2O_3 layer is enhanced by forming a junction with the Fe_2O_3 layer, compared with the result of bulk Cr_2O_3. The long-range correlation is absent above the Néel temperature of Cr_2O_3, and there remains the short-range correlation. The spin correlation in the Cr_2O_3 layer reaches up to $m \sim 20$ [Fig. 4(a) and (b)] in the bilayer systems with split-metal and oxygen-divided interfaces at $T = 1.1\ T_{\rm N}^{\rm Cr_2O_3}$, respectively, whereas the spin correlation in bulk Cr_2O_3 reaches only to $m \sim 10$ [Fig. 4(c)].

To quantify the enhancement of the spin correlation, the correlation length ξ is evaluated in these systems. Fig. 5 shows the temperature dependence of ξ obtained by fitting the spin correlation function into $|\langle \boldsymbol{S}_0 \cdot \boldsymbol{S}_m\rangle_T| = \exp(-x_m/\xi)$ (x_m is

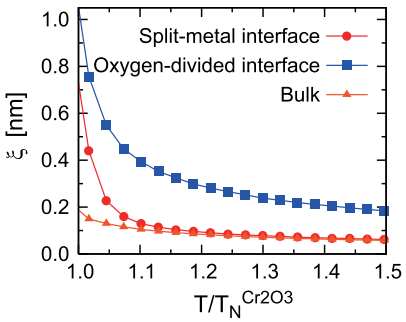

Fig. 5. Temperature dependence of spin correlation length ξ obtained by fitting the spin correlation function shown in Fig. 4.

the position of spin at site m), where the least-square method was used to determine ξ. We set $x_{m+12} - x_m$ to 1.357 nm, which corresponds to the lattice parameter c of the hexagonal unit cell of the corundum-type Cr_2O_3 [23]. The correlation length monotonically decreases with increasing temperature. In the Fe_2O_3/Cr_2O_3 bilayer systems, ξ increases; especially, for the oxygen-divided interface, ξ is more than twice as large as that of the Cr_2O_3 bulk system. This result reveals that the formation of a junction with the Fe_2O_3 layer is a promising approach to enhance the spin correlation in the Cr_2O_3 film.

To enhance the spin correlation in the Cr_2O_3 film more efficiently, the control of the interface structure is important. In Fig. 4, the $|\langle \boldsymbol{S}_0 \cdot \boldsymbol{S}_m \rangle_T|$ values at $m = 1$ and $m = 3$ in the split-metal interface and at $m = 2$ in the oxygen-divided interface decreases drastically. Also, in Fig. 5, the ξ values in the split-metal interface rapidly decrease with increasing temperature compared with that in the oxygen-divided interface. These decrements are attributed to the magnetic frustration. Because of magnetic frustration, the fluctuation of Cr spins at these sites becomes more serious at a finite temperature, and spin correlation becomes small. Because the number of the frustrated Cr site in the oxygen-divided interface is less than that in the split-metal interface, the oxygen-divided interface is more favorable to enhance the spin correlation. Further, if we can design an interface structure with less magnetic frustration, still more enhancements of the spin correlation can be expected.

IV. Conclusion

In summary, we proposed an approach to maintain the antiferromagnetic spin correlation in a thin Cr_2O_3 film above the Néel temperature by forming a junction with the Fe_2O_3 layer. First-principles calculations were performed to evaluate the exchange coupling constants, and Monte-Carlo simulations in the classical Heisenberg model were performed to analyze the spin correlation functions at a finite temperature. We found that the spin correlation in the Cr_2O_3 film can be enhanced by forming a junction with the Fe_2O_3 layer compared with bulk Cr_2O_3. The length of the antiferromagnetic spin correlation in the bilayer system with the oxygen-divided interface above the Néel temperature of Cr_2O_3 is enhanced by twice than that of the bulk system.

Acknowledgment

The authors would like to thank Prof. M. Sahashi, Dr. T. Nozaki, N. Shimomura, T. Ashida (Tohoku University), and Dr. T. Shibata (TDK Corporation) for their valuable discussions and comments. This work was supported by the JST-ALCA.

References

[1] P. Borisov, A. Hochstrat, X. Chen, W. Kleemann, and C. Binek, "Magnetoelectric switching of exchange bias," *Phys. Rev. Lett.*, vol. 94, no. 11, pp. 117203-1–117203-4, Mar. 2005.

[2] X. He *et al.*, "Robust isothermal electric control of exchange bias at room temperature," *Nature Mater.*, vol. 9, no. 7, pp. 579–585, Jul. 2010.

[3] N. Shimomura, K. Sawada, T. Nozaki, M. Doi, and M. Sahashi, "Demonstration of magnetoelectric effect in ultrathin Cr_2O_3/Fe_2O_3 nano-oxide layer by training effect," *Appl. Phys. Lett.*, vol. 101, no. 1, pp. 012403-1–012403-4, Jul. 2012.

[4] X. Chen, A. Hochstrat, P. Borisov, and W. Kleemann, "Magnetoelectric exchange bias systems in spintronics," *Appl. Phys. Lett.*, vol. 89, no. 20, pp. 202508-1–202508-3, Nov. 2006.

[5] M. Bibes and A. Barthélémy, "Multiferroics: Towards a magnetoelectric memory," *Nature Mater.*, vol. 7, pp. 425–426, Jun. 2008.

[6] W. Kleemann, "Magnetoelectric spintronics," *J. Appl. Phys.*, vol. 114, no. 2, pp. 027013-1–027013-3, Jul. 2013.

[7] K. M. Corliss, J. M. Hastings, R. Nathans, and G. Shirane, "Magnetic structure of Cr_2O_3," *J. Appl. Phys.*, vol. 36, no. 3, pp. 1099–1100, Mar. 1965.

[8] S. Mu, A. L. Wysocki, and K. D. Belashchenko, "Effect of substitutional doping on the Néel temperature of Cr_2O_3," *Phys. Rev. B*, vol. 87, no. 5, pp. 054435-1–054435-11, Feb. 2013.

[9] Y. Kota, H. Imamura, and M. Sasaki, "Strain-induced Néel temperature enhancement in corundum-type Cr_2O_3 and Fe_2O_3," *Appl. Phys. Exp.*, vol. 6, no. 11, pp. 113007-1–113007-4, Nov. 2013.

[10] Y. Kota, H. Imamura, and M. Sasaki, "Effect of lattice deformation on exchange coupling constants in Cr_2O_3," *J. Appl. Phys.*, vol. 115, no. 17, pp. 17D719-1–17D719-3, May 2014.

[11] N. J. Mosey, P. Liao, and E. A. Carter, "Rotationally invariant ab initio evaluation of Coulomb and exchange parameters for DFT+U calculations," *J. Chem. Phys.*, vol. 129, no. 1, pp. 014103-1–014103-13, Jul. 2008.

[12] C. W. Searle and G. W. Dean, "Temperature and field dependence of the weak ferromagnetic moment of hematite," *Phys. Rev. B*, vol. 1, pp. 4337–4342, Jun. 1970.

[13] J. Unguris, R. J. Celotta, and D. T. Pierce, "Magnetism in Cr thin films on Fe (100)," *Phys. Rev. Lett.*, vol. 69, no. 7, pp. 1125–1128, Aug. 1992.

[14] F. Maccherozzi *et al.*, "Evidence for a magnetic proximity effect up to room temperature at Fe/(Ga, Mn)As interface," *Phys. Rev. Lett.*, vol. 101, no. 26, pp. 267201-1–267201-4, Dec. 2008.

[15] G. Kresse and J. Furthmüller, "Efficient iterative schemes for ab initio total-energy calculations using a plane-wave basis set," *Phys. Rev. B*, vol. 54, no. 16, pp. 11169–11186, Oct. 1996.

[16] G. Kresse and J. Hafner, "Ab initio molecular dynamics for liquid metals," *Phys. Rev. B*, vol. 47, no. 1, pp. 558–561, Jan. 1993.

[17] E. Krén, P. Szabó, and G. Konczos, "Neutron diffraction studies on the $(1-x)Fe_2O_3$–xRh_2O_3 system," *Phys. Lett.*, vol. 19, pp. 103–104, Oct. 1965.

[18] J. Z. Liu, "Morin transition in hematite doped with iridium ions," *J. Magn. Magn. Matter.*, vols. 54–57, pp. 901–902, Feb. 1986.

[19] J. E. Jaffe, M. Dupuis, and M. Gutowski, "First-principles study of noncommutative band offsets at α-Cr_2O_3 and α-Fe_2O_3 (0001) interfaces," *Phys. Rev. B*, vol. 69, no. 20, pp. 205106-1–205106-7, May 2004.

[20] H. S. Nabi and R. Pentcheva, "Energetic stability and magnetic coupling in $(Cr_{1-x}Fe_x)_2O_3$: Evidence for a ferrimagnetic ilmenite-type superlattice from first principles," *Phys. Rev. B*, vol. 83, no. 21, pp. 214424-1–214424-5, Jun. 2011.

[21] J. Kanamori, "Superexchange interaction and symmetry properties of electron orbitals," *J. Chem. Phys. Solids*, vol. 10, no. 2, pp. 87–98, 1959.

[22] J. B. Goodenough, "Direct cation—cation interactions in several oxides," *Phys. Rev.*, vol. 117, no. 6, pp. 1442–1451, Mar. 1960.

[23] L. W. Finger and R. M. Hazen, "Crystal structure and isothermal compression of Fe_2O_3, Cr_2O_3, and V_2O_3 to 50 kbars," *J. Appl. Phys.*, vol. 51, no. 10, pp. 5362–5367, Oct. 1980.